Eur. Phys. J. E **13**, 99–106 (2004)
DOI: 10.1140/epje/e2004-00044-1

THE EUROPEAN PHYSICAL JOURNAL E

Towards efficient methods for the study of pattern formation in ferrofluid films

J. Richardi and M.P. Pileni[a]

Laboratoire des Matériaux Mésoscopiques et Nanométriques, UMR CNRS 7070, Université Pierre et Marie Curie (Paris VI), BP. 52, 4, place Jussieu, 75230 Paris Cedex 05, France

Received 14 February 2003 / Received in final form 28 October 2003
Published online 2 March 2004 –

Abstract. Hexagonal and labyrinthine patterns appear in thin ferrofluid films after application of a magnetic field perpendicular to the film. The pattern size and the stability of the hexagonal and labyrinthine structures can be predicted by free energy approaches. Several approximations are used in the literature to accelerate the calculation of the magnetic energy. They are usually based on the use of a *uniform*, *average* or *constant* magnetization. In the *uniform* approximation the magnetization at all points in the pattern is assumed to be equal to its value at the center of the stripes or cylinders in the labyrinthine or hexagonal patterns. Recent papers indicate that this approximation gives qualitatively wrong results. This is corroborated here by a comparison with accurate results. When a volume-*averaged* magnetization is used during the calculation of the demagnetization field, from which the magnetic energy is evaluated, the theoretical results are only slightly modified with respect to the accurate results. Thus, we can propose a new method which gives results in good agreement with the accurate values and accelerates the calculations by a factor of 1000. The influence of the approximations is explained by a study of the evolution of the demagnetization field in the patterns. This study indicates that the volume-averaged approximation might only be reliable for patterns with a homogeneously distributed magnetic fluid. Another approximation of a *constant* magnetization, which is widely used in the literature, assumes that the magnetization does not change during the pattern formation in contrast to the *uniform* and *average* approximations. A different way of computing the *constant* magnetization than that usually employed markedly improves the agreement with the accurate results. This is explained by the derivation of a direct relationship between the approximations of a *constant* and an *average* magnetization.

PACS. 47.54.+r Pattern selection; pattern formation – 47.65.+a Magnetohydrodynamics and electrohydrodynamics – 77.84.Nh Liquids, emulsions, and suspensions; liquid crystals

1 Introduction

The formation of patterns is observed in a large variety of physical and chemical systems [1]. In general, simple morphologies of some degree of regularity predominate in two-dimensional systems, e.g., labyrinthine patterns of stripes or hexagonal arrays of bubbles. These patterns appear in type I superconductors subjected to a magnetic field [2] and in micrometric films of ferromagnetic garnets [3]. Stripe and bubble morphologies also arise in Langmuir monolayers [4,5], di-block copolymers [6,7] and physicosorbed monolayers on solid surfaces [8]. Similar patterns appear in ferrofluid films, in which we are interested. Thus, labyrinthine patterns made of stripes and hexagonal arrays of cylinders were observed, when a magnetic fluid is confined with a non-magnetic liquid between two glass plates and a field perpendicular to the plates is applied [9–14]. Recently, we discovered that similar, but solid mesostructures of cobalt nanocrystals are produced, when a solution of these nanocrystals is evaporated while applying a magnetic field [15]. The universality of the observed morphologies arises because, for all systems mentioned, the organized structures are due to a competition of short-range attractive and long-range repulsive forces.

The theoretical study of the patterns in ferrofluid films has attracted much interest [16–22]. Usually, the geometry and dynamics of the pattern formation are studied using free energy approaches. The energy terms for the patterns are now well established and the parameters controlling the structures are known. However, an accurate computation of the free energy is still a difficult task mainly due to the non-uniform magnetization within the ferrofluid pattern. In fact, the magnetization depends on the strength of the demagnetization field, which varies within the pattern.

[a] e-mail: pileni@sri.jussieu.fr

In order to avoid the complicated calculations due to a non-uniform magnetization, two approximations have been widely used in the literature:

- The magnetization is replaced by a *constant* value determined from the applied external field as proposed by Cebers [10]. The variation of the magnetization due to the change in the demagnetization field during the pattern formation is neglected.
- The magnetization at all points in the ferrofluid is calculated from the field at the center of the cylinder or stripe (*uniform* approximation) [11].

Recently, we have shown that the second approximation of a *uniform* magnetization, accurate at a relatively low applied field intensity, is less able to correctly describe the experimental decay of the pattern size as the field is increased to high values [23]. Moreover, the *uniform* approximation predicts that increasing the applied field can lead to a transition between hexagonal and labyrinthine patterns, when the applied field is increased. This is not confirmed by more accurate methods presented in the following. Obviously, an approximate calculation of the magnetic energy can even qualitatively change the theoretical results. It is therefore important to develop reliable, but still efficient methods of computing the magnetic energy. We would like to note that the transition between hexagonal and labyrinthine patterns was experimentally observed by varying the external field [12,14]. The origin of these transitions is not yet completely understood (see discussion in Ref. [24]).

In a previous paper [24], we developed an approach to calculating the magnetic energy using a non-uniform magnetization (called method A). The only approximation is the use of the magnetization *averaged* in the direction of the applied field during the evaluation of the demagnetization field. The magnetization and the magnetic energy are calculated from the approximate demagnetization field.

The aim of this paper is to develop more efficient methods of computing the magnetic energy of ferrofluid patterns. Therefore, we need to understand the influence of the approximations on the theoretical results. Two major approximations are tested:

- an *average* magnetization used during the calculation of the demagnetization field (methods A and A'),
- a *constant* magnetization assumed during the pattern formation (methods C and C').

In methods A, A', C, and C', different ways of calculating the *average* or *constant* magnetization are used. Thus, the influence of the way of computing the magnetization on the theoretical results can be studied. Moreover, this will help us to establish a relationship between both approximation schemes. The results of methods A and C are shown in reference [24] and are presented here for the sake of comparison.

In order to check the quality of the results obtained by the approximate methods, we develop a calculation of the magnetic energy for an idealized labyrinthine pattern without approximations (method A*). To the best of our knowledge, this is the first exact computation of magnetic energies for idealized striped patterns. To provide a comparison, the results obtained by the *uniform* approximation from reference [24] (called method B) are also shown. The differences in the six methods are presented in Table 1. The calculations were carried out using a home–made FORTRAN package [25].

Table 1. Characteristics of the methods of computing the magnetic energy used in this paper. The approximation of the magnetization used to compute the demagnetization field and the equations for the magnetic energy are indicated. The accuracy of the methods is expected to decrease from top to bottom.

method	magnetization used	energy equation
A*	no approximation	Eqs. (1) or (2)
A	*averaged* in the field direction	Eqs. (1) or (2)
A'	*averaged* in all directions	Eqs. (1) or (2)
B	at the center of stripe or cylinder	Eqs. (1) or (2)
C	value before pattern formation	Eq. (9) in [24]
C'	calculated from external field	Eq. (9) in [24]

This paper is structured as follows. In Section 2, we explain the different ways of computing the magnetic energies. In Section 3, we compare the theoretical trends of the pattern size as a function of the applied field predicted by the different methods. The theoretical results are compared to experimental data obtained by Rosensweig et al. [11]. In Section 3.4, the observed differences are interpreted by a study of the spatial evolution of the demagnetization field within the pattern found by the different methods.

2 Theory

2.1 Models of the magnetic pattern

Following the previous study [24], the labyrinth is described by a repeating pattern of infinitely long parallel stripes. The hexagonal pattern is idealized as a hexagonal array of cylinders consisting of the magnetic fluid. In the selected laboratory frame, the x axis is parallel to the direction of the external magnetic field and for the striped pattern, the stripes are along the y axis. The radius of a cylinder is denoted by r_0, while w_f is the width of the labyrinthine stripes. The values of r_0 and w_f corresponding to the free energy minimum are completely determined by the following parameters: the external field H_0, the pattern height L, the magnetic susceptibility χ, the interfacial tension σ and the volume fraction ϕ of the magnetic fluid. The χ and σ values used in the following correspond to the system studied by Rosensweig et al. [11] ($\chi = 1.6$ and $\sigma = 0.0043$ Nm^{-1}). The volume fraction and the cell height are fixed at the values employed in the experiments ($\phi = 0.5$ and $L = 0.9$ mm).

2.2 Free energy functionals of patterns in ferrofluids

In a recent paper [24], we derived the free energy per surface area of hexagonal and labyrinthine patterns in

magnetic fluids:

$$f_h = \phi \left\{ 2\frac{L}{r_0}\sigma - \frac{1}{2}\mu_0 L \langle M \rangle_h H_0 \right\}, \quad (1)$$

$$f_l = \phi \left\{ 2\frac{L}{w_f}\sigma - \frac{1}{2}\mu_0 L \langle M \rangle_l H_0 \right\}. \quad (2)$$

The first term on the right side represents the surface energy. The second term in equations (1, 2) corresponds to the magnetic energy, where $\langle M \rangle_h$ and $\langle M \rangle_l$ are the volume *averaged* magnetization in the hexagonal and labyrinthine patterns, respectively. The derived free energy functionals hold only for a magnetic fluid with a linear relationship between the magnetization and the total field.

2.3 The calculation of the magnetization

From equations (1, 2) it follows that the volume-*averaged* magnetization must be known to obtain estimates of the free energy. Three methods (A, B, and C) have been presented elsewhere [24]. They mainly differ in the way of computing the magnetic energy (Tab. 1). In the following, we restrict ourselves to the new methods A*, A' and C'.

2.3.1 Method A*: accurate approach

The magnetization is calculated by an iterative procedure for a given set of ϕ, χ, H_0, L and σ. It starts with the choice of an arbitrary initial magnetization $\mathbf{M}(\mathbf{r})$. From $\mathbf{M}(\mathbf{r})$ the demagnetization field is calculated using:

$$\mathbf{H}_i(\mathbf{r}) = \int_{V_m} d\mathbf{r'} \frac{1}{4\pi(\mathbf{r'}-\mathbf{r})^3} \left\{ -\mathbf{M}(\mathbf{r'}) + \frac{3[\mathbf{M}(\mathbf{r'})\cdot(\mathbf{r'}-\mathbf{r})](\mathbf{r'}-\mathbf{r})}{(\mathbf{r'}-\mathbf{r})^2} \right\}, \quad (3)$$

$$\mathbf{H}_d(\mathbf{r}) = \sum_i \mathbf{H}_i(\mathbf{r}-\mathbf{r}_i), \quad (4)$$

where $\mathbf{H}_i(\mathbf{r})$ are the fields due to a single stripe or cylinder. $\mathbf{r}_i$ is the position of the center of a stripe or cylinder. V_m denotes the volume occupied by the ferrofluid. A sum of the applied field and the demagnetization field gives the total field

$$\mathbf{H}(\mathbf{r}) = \mathbf{H}_0 + \mathbf{H}_d(\mathbf{r}). \quad (5)$$

A new estimate of the magnetization can be calculated from the equation

$$\mathbf{M'}(\mathbf{r}) = \chi \mathbf{H}(\mathbf{r}). \quad (6)$$

The mixture of $\mathbf{M'}$ and $\mathbf{M}$ is necessary to assure the convergence of the iterative procedure:

$$\mathbf{M"}(\mathbf{r}) = \alpha \mathbf{M}(\mathbf{r}) + (1-\alpha)\mathbf{M'}(\mathbf{r}), \quad (7)$$

where a mixture parameter α of about 0.5 has been employed. If $\mathbf{M'}(\mathbf{r})$ differs from $\mathbf{M}(\mathbf{r})$, the iterative procedure restarts with the calculation of the demagnetization field replacing $\mathbf{M}(\mathbf{r})$ by $\mathbf{M"}(\mathbf{r})$.

The main difficulty is the calculation of the fields $\mathbf{H}_i(\mathbf{r})$ in equation (3). Due to the complex dependence of $\mathbf{M}(\mathbf{r})$ upon $\mathbf{r}$, no analytical form can be obtained for the integrals of equation (3). Moreover, the integrals have an integrable singularity in equation (3) if $\mathbf{r} = \mathbf{r'}$. This singularity can be removed as follows. Two fields $\mathbf{H}_i^{diff}(\mathbf{r})$ and $\mathbf{H}_i^{corr}(\mathbf{r})$ are obtained by replacing $\mathbf{M}(\mathbf{r})$ in equation (3) either by $\mathbf{M}(\mathbf{r'}) - \mathbf{M}(\mathbf{r})$ or by $\mathbf{M}(\mathbf{r})$, respectively.

$$\mathbf{H}_i^{diff}(\mathbf{r}) = \int_{V_m} d\mathbf{r'} \frac{1}{4\pi(\mathbf{r'}-\mathbf{r})^3} \left\{ -(\mathbf{M}(\mathbf{r'}) - \mathbf{M}(\mathbf{r})) + \frac{3[(\mathbf{M}(\mathbf{r'}) - \mathbf{M}(\mathbf{r}))\cdot(\mathbf{r'}-\mathbf{r})](\mathbf{r'}-\mathbf{r})}{(\mathbf{r'}-\mathbf{r})^2} \right\} \quad (8)$$

$$\mathbf{H}_i^{corr}(\mathbf{r}) = \int_{V_m} d\mathbf{r'} \frac{1}{4\pi(\mathbf{r'}-\mathbf{r})^3} \left\{ -\mathbf{M}(\mathbf{r}) + \frac{3[\mathbf{M}(\mathbf{r})\cdot(\mathbf{r'}-\mathbf{r})](\mathbf{r'}-\mathbf{r})}{(\mathbf{r'}-\mathbf{r})^2} \right\}. \quad (9)$$

The sum of $\mathbf{H}_i^{diff}(\mathbf{r})$ and $\mathbf{H}_i^{corr}(\mathbf{r})$ gives $\mathbf{H}_i(\mathbf{r})$. The integrals of $\mathbf{H}_i^{diff}(\mathbf{r})$ are free from singularities, since $\mathbf{M}(\mathbf{r'}) - \mathbf{M}(\mathbf{r})$ goes rapidly to zero as $\mathbf{r'}$ goes to $\mathbf{r}$. In order to control this, the values of the integrand in equation (8) have been numerically calculated. The values indicate that the integrand actually goes to zero as $\mathbf{r'}$ goes to $\mathbf{r}$ and the singularity disappears.

The new integrals in equation (8) can therefore be calculated by numerical techniques as explained below. The integrals of $\mathbf{H}^{corr}(\mathbf{r})$, for which $\mathbf{M}(\mathbf{r'})$ is replaced by the constant $\mathbf{M}(\mathbf{r})$ can be solved analytically, which gives, in the case of the striped pattern, e.g., for $H_{i,x}^{corr}$:

$$H_{i,x}^{corr}(\mathbf{r}) = \frac{M_x(\mathbf{r})}{2\pi} \left\{ \arctan\left(\frac{x_u}{z_u}\right) - \arctan\left(\frac{x_u}{z_l}\right) - \arctan\left(\frac{x_l}{z_u}\right) + \arctan\left(\frac{x_l}{z_l}\right) \right\} - \frac{M_z(\mathbf{r})}{4\pi} \left\{ \ln \frac{(x_u^2+z_u^2)(x_l^2+z_l^2)}{(x_u^2+z_l^2)(x_l^2+z_u^2)} \right\} \quad (10)$$

where $x_u = L/2 - x$, $x_l = -L/2 - x$, $z_u = w_f/2 - z$ and $z_l = -w_f/2 - z$.

Due to the symmetry of the labyrinthine patterns, we can restrict ourselves to the calculation of $\mathbf{H}_i(\mathbf{r})$ for varying x and z keeping $y/L = 0$. Moreover, the y elements of $\mathbf{H}_i(\mathbf{r})$ are zero and, therefore, need not be computed. Nevertheless, we have to calculate the three-dimensional integrals of equation (3) in the two dimensions x and z, which is very time-consuming. The computing time was drastically reduced with the help of two numerical techniques [27]. First, an exponential grid is used in the z direction, which greatly reduces the number of points at which the fields must be calculated. Second, the integrals were calculated using the Romberg method [27]. This is an extrapolation method based upon the trapezoidal rule.

Thus, the number of integration steps is adapted for every integral to reach an initially fixed numerical precision. This technique allows very precise evaluations of the integrals at low computational costs. An alternative method would be the use of the Fourier transform to handle the convolution integrals of equation (3). However, a gain in computing time implies the use of the Fast-Fourier transform method, which is based upon a trapezoidal rule. In contrast to the Romberg method, the use of the trapezoidal rule does not include a control of the numerical precision for the calculated integrals. As we aim at high accuracy, the application of the Fourier transform is not possible in our case.

Due to the long range of dipolar interactions, the sum in equation (4) cannot be simply cut off at a large distance. In paper [24] we derived a correct treatment of these long-range interactions, which is used here.

2.3.2 Method A': volume-averaged magnetization

Method A' is similar to approach A (*average* magnetization in the field direction) presented in article [24]. It is introduced with the aim of obtaining a faster method than A with still reliable results. As in method A, its only approximation is the use of an *average* magnetization in calculating the demagnetization field within the pattern. But in contrast to method A, the magnetization is *averaged* in all directions. Therefore, method A' is expected to be less accurate than method A* (no averaging) and A (averaging only in the field direction).

The volume-*averaged* value $\langle \mathbf{M} \rangle$ is used to replace $\mathbf{M}(\mathbf{r})$ in the computation of $\mathbf{H}_i(\mathbf{r})$ in equation (3). Due to the symmetry of the idealized patterns, the y and z elements of $\langle \mathbf{M} \rangle$ are zero and all terms depending on M_y or M_z vanish. Moreover, $\langle M_x \rangle$ does not depend on $\mathbf{r}$ and can be excluded from the integrals in equation (3). The calculation of the demagnetization field in equations (3, 4) can then be largely simplified:

$$I_{i,x}(\mathbf{r}) = \int_{V_m} \frac{d\mathbf{r'}}{4\pi(\mathbf{r'}-\mathbf{r})^3} \left\{ -1 + \frac{3(x'-x)^2}{(\mathbf{r'}-\mathbf{r})^2} \right\}, \tag{11}$$

$$D = -\left\langle \sum_i I_{i,x}(\mathbf{r}-\mathbf{r}_i) \right\rangle, \tag{12}$$

$$\langle H_d \rangle = -D \langle M \rangle . \tag{13}$$

where D is the demagnetization factor.

Using equations (5, 6), we arrive at the following relationship for the *average* magnetization:

$$\langle M \rangle = \frac{\chi H_0}{1+\chi D}. \tag{14}$$

The integrals in equation (11) can be solved analytically in all three directions. In the case of the hexagonal pattern, this leads to ellipsoidal functions [3]. D depends only on the pattern size r_0 or w_f and on the volume fraction ϕ. For given values of ϕ and r_0 or w_f, D can be calculated and stored. Then, during the iterative procedure and for different field strengths, the new magnetization can be evaluated from the stored values of D using equation (14). Therefore, this approximation is computationally extremely fast.

2.3.3 Method C': constant magnetization

Method C is explained in detail in our previous paper [24]. The difference between the two methods (C and C') is the way of computing the *constant* magnetization. In method C, the magnetization is calculated from its value observed before the pattern formation.

$$\mathbf{M} = \frac{\mathbf{M}_{\text{init}}}{\phi} = \frac{\chi \mathbf{H}_0}{1+\chi\phi}, \tag{15}$$

where $\mathbf{M}_{\text{init}} = \chi_{\text{init}}(\mathbf{H}_0 + \mathbf{H}_{d,\text{init}})$, $\chi_{\text{init}} = \phi\chi$ and $\mathbf{H}_{d,\text{init}} = -\mathbf{M}_{\text{init}}$.

In method C', the magnetization is evaluated as proposed in the literature [10]

$$\mathbf{M} = \chi \mathbf{H}_0. \tag{16}$$

We study methods C and C', because they have been widely used [18–21].

The magnetic terms in equations (1, 2) are only valid when the magnetization varies with the change in the demagnetization field caused by the pattern formation. Due to the assumption of a constant magnetization, this is not the case in methods C and C'. Therefore, the magnetic energy must be calculated from the repulsion between the aligned magnetic dipoles as explained in detail in reference [24].

3 Results

3.1 Agreement between experiment and the accurate results

In Figure 1, the energetically favorable stripe width in a labyrinthine pattern is plotted as a function of the applied field according to methods A*, A and A'. The dots are the experimental data points obtained from reference [11] (see details in Ref. [23]). At low field, the calculated pattern size obtained by the accurate method A* is too large in comparison with experiment. At higher field strengths, method A* correctly reproduces the experimental decay of the stripe width. It is somewhat surprising that an approach based upon a linear relationship between the magnetization and the field yields correct predictions even at high fields. In order to understand this, we carried out a study modeling the magnetization curve by a non-linear Langevin curve. The magnetic energy cannot be calculated using the second term in equations (1, 2), since it is valid only in the linear case. The general equation for the magnetic energy must be used. Details of the calculations

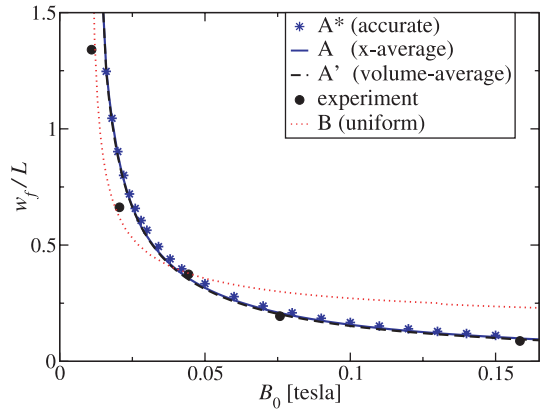

Fig. 1. Dependence of the normalized stripe width w_f/L in labyrinths on the external field H_0. The theoretical results of methods A*, A, A' and B are compared to experimental data. The cell height and volume fraction are fixed at $L = 0.9$ mm and at $\phi = 0.5$. The experimental points were obtained from reference [11].

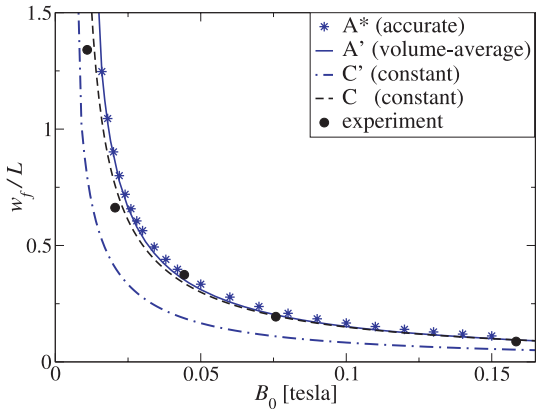

Fig. 2. Dependence of the normalized stripe width w_f/L in labyrinths on the external field B_0. The results of the methods A*, A', C and C' are compared to experimental data obtained from reference [11]. The parameters correspond to those used for Figure 1.

are published elsewhere [28]. The preliminary results indicate that the agreement between the linear and the nonlinear curves markedly depends on the particle size. For a particle diameter of 10 nm the non-linear curve deviates from the linear one for field strengths larger than 0.05 tesla. In contrast, for a smaller particle diameter of 6 nm the linear and nonlinear curves coincide. Since Rosensweig et al. did not mention the size of particles used, it is difficult to explain why the linear theory gives results in agreement with the experimental data.

3.2 The influence of the approximation of an average magnetization on the theoretical results

The curves obtained by methods A and A' deviate only slightly from that calculated by the accurate approach. Obviously, the use of an *average* magnetization during the evaluation of the demagnetization field does not markedly affect the theoretical results. This can be understood by comparing the magnetic energies obtained by the different methods. The magnetic energies calculated by methods A and A' deviate by about 1% from the exact values. This should be compared to the energy differences of about 5% caused by the approximations of method B. Indeed, B gives stripe widths which are quite different from approach A* (see Fig. 1). To understand the good agreement between methods A*, A, and A' and the deviations caused by method B, we have to consider the spatial evolution of the demagnetization field calculated from the different methods (see Sect. 3.4). The demagnetization field is used to calculate the magnetization, which gives the magnetic energy according to equations (1, 2). Thus, a comparison of the demagnetization fields can explain the differences in the magnetic energies observed for the various approximations.

In paper [24], we compared the transitions between hexagonal and striped patterns predicted by methods A, B, and C. For this purpose, the evolution of the energy difference between both patterns with the field strength and the phase ratios has been calculated. The energy differences obtained by method A' are very close to those of A, although a different way of averaging the magnetization was employed. We conclude that the use of an *average* magnetization during the evaluation of the demagnetization fields does not markedly affect the theoretical results.

3.3 The influence of the approximation of a constant magnetization on the theoretical results

The curve in Figure 2 calculated by method C is close to that of the exact method (A*). At first sight, this agreement is surprising, because method C explains the pattern formation by a different mechanism (see article [24]). We can explain the agreement by establishing a relationship between methods A' and C. Using equation (14), the magnetic energy per surface area for method A' can be written as:

$$f_{m,\mathrm{A}'} = -\frac{\mu_0}{2}\frac{\chi H_0^2}{1+\chi D}\phi L. \tag{17}$$

In method C, the magnetic energy is given by [24]:

$$F_{m,\mathrm{C}} = \frac{\mu_0}{2}\int \mathbf{H}_d(\mathbf{r})\cdot\mathbf{H}_d(\mathbf{r})d\mathbf{r} = -\frac{\mu_0}{2}\int_{V_m} M\mathbf{H}_d(\mathbf{r})d\mathbf{r}. \tag{18}$$

Using equations (13) and (15), we arrive at the following expressions for the magnetic energy per surface area:

$$f_{m,\mathrm{C}} = \frac{\mu_0}{2}\frac{\chi^2 H_0^2}{(1+\chi\phi)^2}D\phi L. \tag{19}$$

For the minimization of the energy, equations (17) and (19) must be derived with respect to the pattern size.

In the labyrinthine case, we obtain

$$\frac{\partial f_{m,\mathrm{A}'}}{\partial w_f} = \frac{\mu_0}{2}\frac{\chi^2 H_0^2}{(1+\chi D)^2}\frac{\partial D}{\partial w_f}\phi L, \tag{20}$$

$$\frac{\partial f_{m,\mathrm{C}}}{\partial w_f} = \frac{\mu_0}{2}\frac{\chi^2 H_0^2}{(1+\chi \phi)^2}\frac{\partial D}{\partial w_f}\phi L. \tag{21}$$

Obviously, the only difference between methods A' and C is that the factor D is replaced by ϕ in the numerator. D ranges between ϕ and 1.0, where $D = 1.0$ corresponds to a closed ferrofluid film ($w_f = \infty$). For the limit $w_f \longrightarrow 0$, the demagnetization coefficient D should be equal to that of a hypothetical homogeneous mixture of the magnetic and the non-magnetic fluids, which can be computed from $D = \phi$ [23]. Therefore, methods C and A' are expected to give the same results at large pattern size (high field), while these should deviate at smaller w_f. This is observed in Figure 2. The same arguments also apply in the hexagonal case (Fig. 3). The comparison of the values obtained by methods C and C' shows that the way of computing M can completely change the results. In particular, method C', widely used in the literature, is not able to reproduce the accurate results. The deviations between the results of C and C' are due to large differences in the magnetic energies. A comparison of equations (15, 16) explains these differences. For $\phi = 0.5$ and $\chi = 1.6$, the magnetization calculated by method C' is larger than that of method C by a factor $1 + \chi\phi = 1.8$. Since the magnetic energy increases with M^2, the f_m obtained by method C' are 3.2 times larger than the values of C. As shown above, the way of computing the magnetization in method C can be justified by a comparison with approach A', which is not the case for method C'.

The evolution of the stripe width as a function of H_0 has also been studied for a value of $\phi = 0.2$. In this case, we can draw the same general conclusions as before.

We have also compared the calculated pattern size obtained by the different methods for the hexagonal case. Due to the lower symmetry of this structure with respect to the striped case, the calculations for the accurate methods are extremely time-consuming. Therefore, we restricted the comparisons to methods A, A', B, C and C'. Figure 3 shows the evolution of the reduced cylinder radius r_0/L with the applied field. We can draw the same conclusion as in the striped case. Therefore, we expect the results of methods A and A' to be close to the accurate values as in Figure 1. The similarity between the calculated results for the hexagonal and striped cases was noted in the previous paper [24], where it was attributed to the same form of the free energy found for both patterns (see Eqs. (1, 2)).

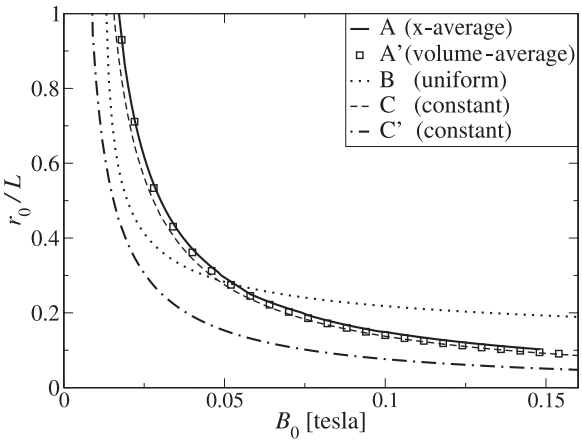

Fig. 3. Dependence of the normalized cylinder radius r_0/L in hexagonal patterns on the external field B_0. The theoretical results of methods A, A', B, C and C' are compared. The parameters are: $\chi = 1.6$, $\phi = 0.5$, $L = 1$ mm, and $\sigma = 0.0043$ Nm^{-1}.

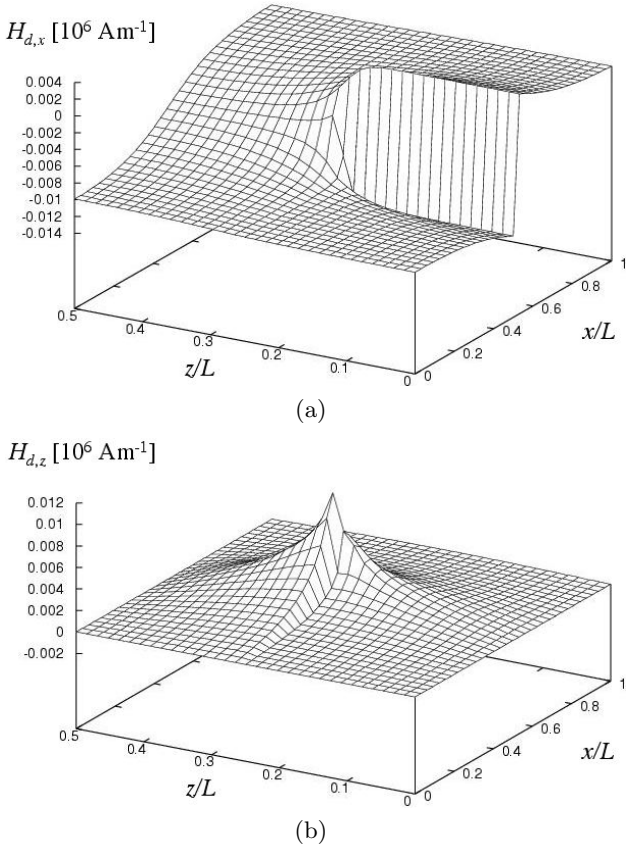

Fig. 4. Evolution of the demagnetization field in a labyrinthine stripe. (a) x element and (b) z element of $\mathbf{H}_d$. (method A*, $\chi = 1.6$, $\phi = 0.5$, $B_0 = 0.03$ tesla and $w_f/L = 0.5$).

3.4 Study of the demagnetization field

In order to understand the influence of the various approximations upon the calculated results, we compare the demagnetization field calculated by the different approaches. First, the spatial evolution of the demagnetization field in a labyrinthine stripe is interpreted using classical magnetostatics. Figures 4a and 4b present the x and z elements of the demagnetization field calculated by the iterative method without any approximation corresponding to approach A*. As explained above, the demagnetization field does not depend on y. Due to the symmetry, the plot can

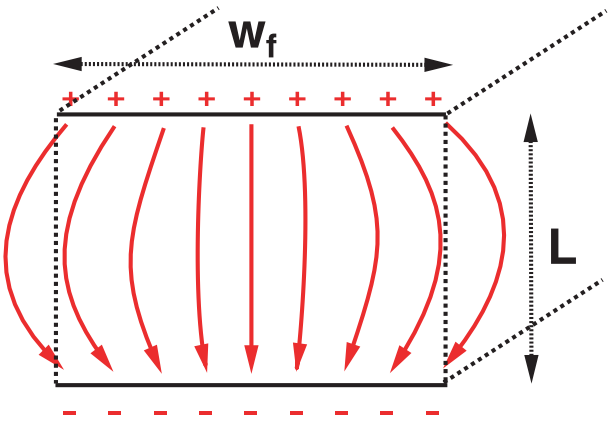

Fig. 5. Sketch of the field lines between two charged planes.

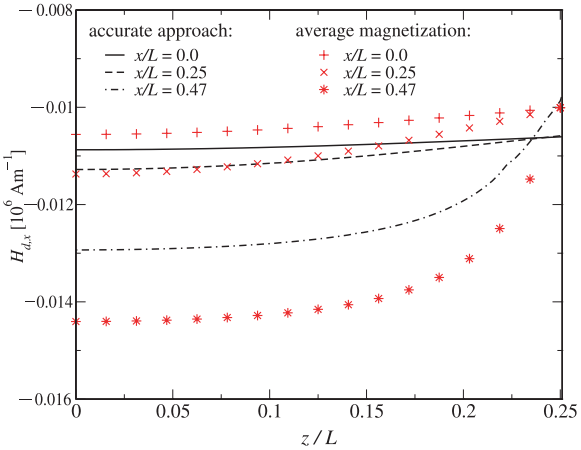

Fig. 6. Field $H_{d,x}$ calculated by methods A* and A'.

be restricted to the upper left quarter of the x-z plane. The point $(x = 0, z = 0)$ is the center of the stripe. The side of the stripe is at $z/L = 0.25$, while the points at $x/L = 0.5$ correspond to the top of the stripe. The discontinuities of $H_{d,x}$ and $H_{d,z}$ at the boundaries of the stripe can be explained by the condition of a continuous normal component for $\mathbf{B}$ at the interface between two magnetic media (see Jackson [26], page 213). To understand the overall spatial evolution of $H_{d,x}$ and $H_{d,z}$, we study the simplified case of a uniform magnetization. The magnetization can be represented as monopoles at the ends of the stripe with the surface charge $\mu_0 M$, as shown in Figure 5. The lines in Figure 5 present the direction of the magnetic field induced by the magnetic charges at both ends of the stripe. From this sketch, we expect $H_{d,z}$ to be large in the stripe corners, whereas it should vanish for $x/L = 0$ or $z/L = 0$. This intuitive picture is confirmed by Figure 4b, which shows a peak in $H_{d,z}$ at the corner of the stripe. Also the fact that $H_{d,x}$ is less negative in the corners is in good agreement with our sketch in Figure 5.

The fields $H_{d,x}$ calculated by methods A* and A' are compared in Figure 6. The parameters correspond to Figure 4. The fields are presented for three different heights x/L. In Section 3.2 we have shown that methods A* and A' give very similar theoretical results. This is caused by the small differences between the average magnetizations calculated by both approaches (for Fig. 6: $\langle M \rangle = 20191$ Am^{-1} for method A*, 20016 Am^{-1} for A' and 20714 Am^{-1} for B). The average magnetization is calculated from

$$\langle M \rangle = \frac{1}{V_m} \int_{V_m} M_x(\mathbf{r}) d\mathbf{r}, \tag{22}$$

$$M_x(\mathbf{r}) = \chi(H_0 + H_{d,x}(\mathbf{r})). \tag{23}$$

According to these equations, the agreement of $\langle M \rangle$ obtained by methods A* and A' can have two different reasons. It might be due to the fact that the demagnetization field calculated using an *average* magnetization is close to the accurate results. This is in contradiction with the curves in Figure 6, which show large differences between the $H_{d,x}$ of both approaches. In particular, close to the top of the stripe ($x/L = 0.47$), approach A' underestimates the demagnetization field by about 10%. The agreement between approaches A* and A' is obviously due to a fortuitous compensation of errors in $H_{d,x}$ during the averaging in equation (22). Indeed, Figure 6 shows that the demagnetization field obtained by method A' is larger than the accurate results in the center of the stripe ($x/L = 0$), whereas it is more negative close to the top ($x/L = 0.47$). The differences between $H_{d,x}$ calculated by both methods can be explained as follows. Let us examine $H_{d,x}$ close to the top of the stripe. The demagnetization field is more negative than in the rest of the stripe. According to equation (23), this leads locally to a decrease in the magnetization with respect to its average value. The locally smaller magnetization gives a less negative $H_{d,x}$ at $x/L = 0.47$ than the values calculated from the larger average magnetization. This agrees with the results shown in Figure 6. In the center of the stripe, the differences in $H_{d,x}$ are interpreted by the inverse effect, which leads to the cancellation of errors mentioned above. Figure 6 helps to understand the failure of method B. The demagnetization field in the center is less negative than the values in the rest of the stripe. Using $H_{d,x}(\mathbf{0})$ to calculate $\langle M_x \rangle$ cannot give reasonable results, because no compensation occurs as in methods A' or A.

4 Conclusions

In a previous paper [24] we found that the approximation of a *uniform* magnetization can lead to qualitatively wrong theoretical results. In a recently published paper, we also show that this approximation predicts the wrong order of transition for the pattern formation at low field strength [29]. Here, the failure of this approach is related to the use of the demagnetization field at the center to calculate the average magnetization. In contrast, an *average* magnetization can be used to calculate the demagnetization field as in methods A' and A. In particular, the new approach A', which is based on a volume *averaged* magnetization, is much faster than the accurate calculation

(method A*) . Thus, the calculation of one energy value is reduced from one hour to a few seconds by the approximation of an *average* magnetization. The good performance of this approach is due to a compensation of errors in the demagnetization field. However, it is very risky to use this approximation under conditions, where a compensation of errors does not operate correctly. This might occur for systems where the magnetic fluid is not homogeneously distributed between the plates. Such systems were studied, e.g., in references [16–19]. For the study of these systems a *constant* magnetization was assumed (method C'). Our results indicate that this approximation does not correctly reproduce the size of pattern due to an incorrect calculation of the magnetization. However, the results do not show qualitatively wrong behavior such as the use of a *uniform* magnetization (method B), which confirms the results obtained using a *constant* magnetization in the literature. We suggest using equation (15) which gives a better agreement with the accurate results (method C). This has been explained by establishing a relationship between methods using an *average* and a *constant* magnetization. However, the use of a *constant* magnetization is also based on the approximation of a uniform magnetization which should fail for in-homogeneously distributed systems studied in references [16–19]. Therefore, further investigations would be of interest to see if the dynamic results published using a *constant* magnetization are still valid using more accurate methods of calculating the magnetic energy.

The authors gratefully acknowledge the contribution of David Portehault to this work. We also like to thank Dr. D. Ingert and V. Germain for fruitful discussions.

References

1. M. Seul, D. Andelman, Science **267**, 476 (1995)
2. R.P. Huebner, *Magnetic Flux Structures in Superconductors* (Springer-Verlag, Berlin, 1979)
3. J.A. Cape, G.W. Lehman, J. Appl. Phys. **42**, 5732 (1971)
4. R.M. Weis, H.M. McConnell, Nature **310**, 47 (1984)
5. H.M. McConnell, Annu. Rev. Phys. Chem. **42**, 171 (1991)
6. E.N. Thomas, D.M. Anderson, C.S. Henke, D. Hoffmann, Nature **334**, 589 (1988)
7. H. Hasegawa, T. Hashimoto, Polymer **33**, 475 (1992)
8. K. Kern, H. Niehus, A. Schatz, P. Zeppenfeld, J. Goerge, G. Comsa, Phys. Rev. Lett. **67**, 855 (1991)
9. R.E. Rosensweig, *Ferrohydrodynamics* (Dover Publications, Mineola, 1997)
10. A. Cebers, M.M. Maiorov, Magnetohydrodynamics **16**, 21 (1980)
11. R.E. Rosensweig, M. Zahn, R. Shumovich, J. Magn. Magn. Mater. **39**, 127 (1983)
12. J.-C. Bacri, R. Perzynski, D. Salin, Endeavour, New Series **12**, 76 (1988)
13. F. Elias, C. Flament, J.-C. Bacri, S. Neveu, J. Phys. I France **7**, 711 (1997)
14. C.-Y. Hong, I.J. Jang, H.E. Horng, C.J. Hsu, Y.D. Yao, H. C. Yang, J. Appl. Phys. **81**, 4275 (1997)
15. J. Legrand, A.T. N'Go, C. Petit, M.P. Pileni, Adv. Mater. **18**, 53 (2001)
16. S.A. Langer, R.E. Goldstein, D.P. Jackson, Phys. Rev. A **46**, 4894 (1992)
17. A.J. Dickstein, S. Erramilli, R.E. Goldstein, D.P. Jackson, S.A. Langer, Science **261**, 1012 (1993)
18. D.P. Jackson, R.E. Goldstein, A.O. Cebers, Phys. Rev. E **50**, 298 (1994)
19. A. Cebers, I. Drikis, Magnetohydrodynamics **32**, 11 (1996)
20. I. Drikis, J.-C. Bacri, A. Cebers, Magnetohydrodynamics **35**, 203 (1999)
21. F.M. Ytreberg, S.R. McKay, Phys. Rev. E **61**, 4107 (2000)
22. D. Lacoste, T.C. Lubensky, Phys. Rev. E **64**, 041506 (2001)
23. J. Richardi, D. Ingert, M.P. Pileni, J. Phys. Chem. B **106**, 1521 (2002)
24. J. Richardi, D. Ingert, M.P. Pileni, Phys. Rev. E **66**, 046306 (2002)
25. The Fortran package $\mathcal{HEXALAB}$ is a highly optimized code of about ten thousands statements, which calculate the geometry and energy of magnetic fluid patterns. The type of patterns are not restricted to hexagonal or labyrinthine ones. $\mathcal{HEXALAB}$ was developed by J. Richardi at the LMN2 (direction: M.P. Pileni)
26. J.D. Jackson, *Classical Electrodynamics*, 3rd edn. (John Wiley & Sons, New York, 1998)
27. W.H. Press, B.P. Flannery, S.A. Teukolsky, W.T. Vetterling, *Numerical Recipes: The Art of Scientific Computing* (Cambridge University Press, Cambridge, 1986)
28. J. Richardi, M.P. Pileni, Phys. Rev. E **69**, 016304 (2004)
29. J. Richardi, M.P. Pileni, Prog. Theor. Chem. Phys. **12**, 41 (2003)